

Quercetin Induces Apoptosis via the Mitochondrial Pathway in KB and KBv200 Cells

Jian-ye Zhang,^{†,‡} Tao Yi,[†] Jing Liu,[†] Zhong-zhen Zhao,[†] and Hu-biao Chen^{*†}

[†]School of Chinese Medicine, Hong Kong Baptist University, Kowloon Tong, Kowloon, Hong Kong

[‡]School of Pharmaceutical Sciences, Guangzhou Medical University, Guangzhou 510182, People's Republic of China

ABSTRACT: In this study, anticancer activities of six compounds of flavonoids were investigated in human epidermoid carcinoma KB and KBv200 cells. Among these compounds, quercetin and acacetin showed strong inhibition of cell growth in KB and KBv200 cells. IC₅₀ values of quercetin against KB and KBv200 cells were 17.84 ± 4.14 and 18.94 ± 4.75 μM, respectively. The IC₅₀ values of acacetin against KB and KBv200 cells were 41.33 ± 6.05 and 49.04 ± 3.64 μM. The IC₅₀ values of apigenin, kaempferol, kaempferol 3-O-rhamnoside, and quercetin 3-O-rhamnoside were more than 100 μM. Furthermore, quercetin was found to induce apoptosis in KB and KBv200 cells via the mitochondrial pathway, including a decrease of the reactive oxygen species level, loss of mitochondrial membrane potential, release of cytochrome *c*, activation of caspase-9 and caspase-3, and cleavage of poly (ADP-ribose) polymerase. The apoptosis induced by quercetin was not related to the regulation of Bcl-2 or Bax in KB and KBv200 cells.

KEYWORDS: flavonoids, quercetin, anticancer, apoptosis, mitochondrial pathway

■ INTRODUCTION

Recently, there has been a dramatic increase in the investigation of naturally occurring products in terms of their potential for treating cancers.¹ One promising group of natural products for cancer therapy is the flavonoids. Multiple epidemiological studies have reported that diets rich in flavonoids can reduce the incidence of various cancers, probably by playing a role in the prevention of cancer, which is related to their antioxidant capacity.^{2,3} Flavonoids are universally present in fruits, cereals, legumes, vegetables, nuts, seeds, herbs, spices, roots, stems, and flowers.^{4,5} For example, quercetin is in the content of many vegetables and fruits, such as mango, apple, pear, grape, cherry, onion, and carrot.⁶

Six flavonoids were isolated and identified in our previous study.^{7–9} These compounds are apigenin (1), acacetin (2), kaempferol (3), quercetin (4), kaempferol 3-O-rhamnoside (5), and quercetin 3-O-rhamnoside (quercitroside, 6) (Figure 1). They are flavones (compounds 1 and 2), flavonols (compounds 3 and 4), and glycosides (compounds 5 and 6).

Herein, the anticancer activities of the above compounds *in vitro* against KB and KBv200 cells were reported. KBv200 cells were cloned from drug-sensitive parental KB cells by stepwise exposure to increasing doses of vincristine (VCR) and ethylmethane sulfonate (EMS) mutagenesis. KBv200 cells were a classic multi-drug resistant (MDR) cell line overexpressing P-glycoprotein (P-gp, ABCB1). KB and KBv200 cells were a typical pair of sensitive and MDR cells for research.¹⁰ We hope to find anticancer agents that are effective in both sensitive and MDR cancer cells. Also, the related mechanism involving the apoptosis induced by quercetin was investigated, which showed the most potent inhibition of cell growth in KB and KBv200 cells.

■ MATERIALS AND METHODS

Chemicals and Reagents. 3-(4,5-Dimethyl-2-thiazolyl)-2,5-diphenyl-2*H*-tetrazolium bromide (MTT), 3,3'-dihexyloxycarbocyanine iodide [DiOC6(3)], and 2',7'-dichlorofluorescein diacetate (DCFH-DA) were purchased from Sigma Chemical Co. Antibodies against caspase-3, caspase-9, and poly (ADP-ribose) polymerase (PARP) were obtained from Signalway Antibody Co., Ltd. Antibodies against cytochrome *c*, Bax, and Bcl-2 were purchased from Santa Cruz Biotechnology Co. Antibodies against GAPDH, anti-mouse immunoglobulin G-horseradish peroxidase (IgG-HRP), and anti-rabbit IgG-HRP were purchased from KangChen Biotechnology Co. (Shanghai, China). All tissue culture supplies were purchased from Gibco-BRL Co. Annexin V-FITC/PI Kit was from KeyGEN Biotech, China. Other routine laboratory reagents were obtained from commercial sources of analytical or HPLC grade. Investigated compounds had a purity of more than 98%.

Cell Lines and Cell Culture. KB cells are human epidermoid carcinoma cell lines. KBv200 cells, a classic MDR cell line overexpressing P-glycoprotein (P-gp, ABCB1), were cloned from drug-sensitive parental KB cells by stepwise exposure to increasing doses of vincristine (VCR) and ethylmethane sulfonate (EMS) mutagenesis. In comparison to KB cell line, the KBv200 cell line was approximately 100 times more resistant to VCR. KB and KBv200 cells were maintained in RPMI 1640 medium containing 100 units/mL penicillin, 100 μg/mL streptomycin, and 10% fetal bovine serum (FBS). All cells were grown in a humidified atmosphere incubator of 5% CO₂ and 95% air at 37 °C.¹⁰

Cell Viability Assay. Cells were harvested during the logarithmic growth phase and seeded in 96-well plates at a density of 1.5 × 10⁴ cells/mL in a final volume of 190 μL/well. After 24 h of incubation, 10 μL of tested compounds at different concentrations was added to 96-well plates. The tested compounds were dissolved in dimethyl sulfoxide (DMSO) and diluted by medium with the ratio of DMSO/

Received: December 9, 2012

Revised: February 13, 2013

Accepted: February 14, 2013

Published: February 14, 2013

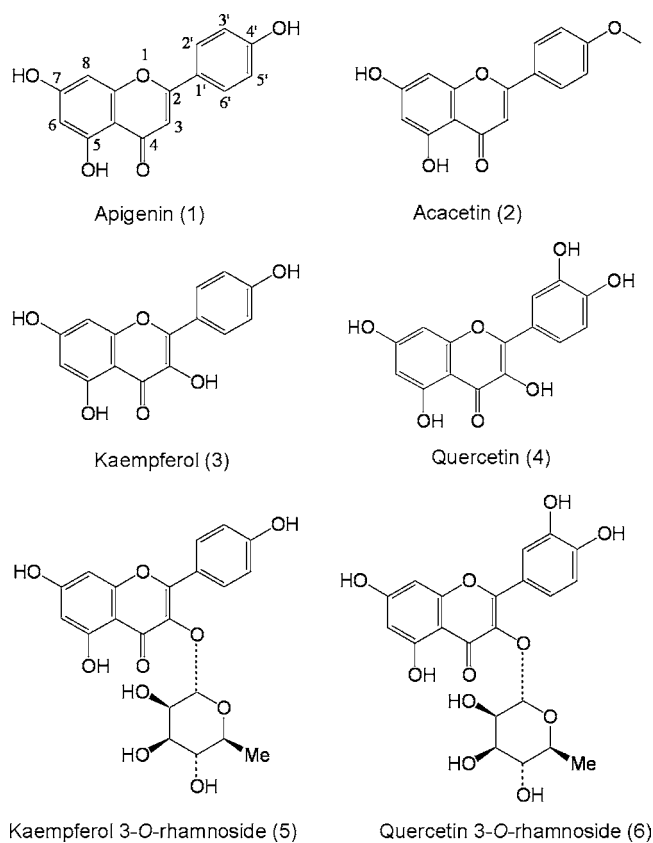


Figure 1. Chemical structures of apigenin (1), acacetin (2), kaempferol (3), quercetin (4), kaempferol 3-O-rhamnoside (5), and quercetin 3-O-rhamnoside (6).

medium less than 1% (v/v). After 68 h of treatment without change of the culture medium, 10 μ L of MTT (10 mM stock solution of saline) was added to each well and culture was continued for 4 h. Subsequently, the supernatant was removed, and MTT crystals were solved with 100 μ L of anhydrous DMSO for each well. Thereafter, optical density was measured by a model 550 microplate reader at 540 nm, with 655 nm as the reference filter. Experiments were performed at least 3 times. The 50% inhibitory concentration (IC_{50}) was determined as the anticancer drug concentration, causing 50% reduction in cell viability and calculated from the curves (Bliss's software). Cell survival was calculated using the following formula: survival (%) = (mean experimental absorbance/mean control absorbance) \times 100%.¹¹ The control wells were not treated with tested compounds.

Annexin V-FITC/PI Double-Staining Assay. Annexin V and PI double-staining was performed with a detection kit. After 5×10^5 cells/well were seeded to a 6-well plate for 24 h, the cells were then treated with quercetin for 12 or 24 h. After that, both floating and attached cells were collected, washed twice with ice-cold phosphate-buffered saline (PBS), and resuspended in 500 μ L of 1 \times binding buffer containing Annexin V-FITC (1:50 solution according to the instructions of the manufacturer) and 40 ng/sample PI for 15 min at 37 $^{\circ}$ C in the dark. Then, the numbers of viable, apoptotic, and necrotic cells were quantified by flow cytometer (BD FASCanto) and analysis by the CellQuest software. At least 10 000 cells were analyzed for each sample. The percent apoptosis (%) = (number of apoptotic cells/number of total cells observed) \times 100%.¹²

Measurement of Reactive Oxygen Species (ROS) Generation. DCFH-DA can be deacetylated by intracellular esterase to the non-fluorescent DCFH, which can be oxidized by ROS to the fluorescent compound 2',7'-dichlorofluorescein (DCF). The fluorescence intensity of DCF is proportional to the amount of ROS produced by the cells. After 5×10^5 cells/well were seeded to a 6-well

plate for 24 h, the cells were treated with quercetin for 24 h. Then, 5×10^5 cells were harvested, washed once with ice-cold PBS, and incubated with DCFH-DA (50 μ M in a final concentration) at 37 $^{\circ}$ C for 30 min in the dark. Then the cells were washed twice and maintained in 1 mL of PBS. The ROS generation was assessed from 10 000 cells from each sample by a BD FASCanto flow cytometer at an excitation wavelength of 488 nm and an emission wavelength of 530 nm. The data of DCF fluorescence intensity were evaluated by CellQuest software and expressed as mean fluorescence intensity (MFI). The experiments were performed at least 3 times.¹⁰

Determination of Mitochondrial Membrane Potential ($\Delta\Psi_m$). $\Delta\Psi_m$ was measured by flow cytometry with the mitochondrial tracking fluorescent DiOC6(3). The cationic lipophilic fluorochrome DiOC6(3) is a cell-permeable marker that specifically accumulates into mitochondria depending upon $\Delta\Psi_m$. After 5×10^5 cells/well were seeded to a 6-well plate for 24 h, the cells were treated with quercetin for 24 h. Then, cells were harvested, centrifuged at 110g for 5 min, and washed with ice-cold PBS once. Consequently, cells were incubated with 40 nM DiOC6(3) at 37 $^{\circ}$ C for 20 min in the dark. Then, the cells were washed twice, resuspended in 1 mL PBS, and analyzed by a BD FASCanto flow cytometer with an excitation wavelength of 484 nm and an emission wavelength of 501 nm. At least 10 000 cells were determined for each sample. The data obtained from flow cytometry were analyzed by CellQuest software and expressed as MFI. The expressed data were the results of three independent determinations.¹¹

Whole-Cell Lysates and Western Blot Analysis. After 3.5×10^6 cells/well were plated to a culture dish (100 \times 20 mm) for 24 h, the cells were treated for 48 h. Then, cells were harvested and washed twice with ice-cold PBS. Subsequently, 1.5 mL of eppendorff containing cells was centrifuged at 110g for 5 min to discard the supernatant. The pellet was vortexed, and 100 μ L of 1 \times loading buffer [50 mM Tris-Cl (pH 6.8), 10% glycerol, 2% sodium dodecyl sulfate, 0.25% bromphenol blue, and 0.1 M dithiothreitol (DTT)] for every 5×10^6 cells was added. After heating at 100 $^{\circ}$ C for 20 min, the lysates in the eppendorff were centrifuged at 15000g for 10 min and the supernatant was collected. An equal amount of lysate protein was separated on 8–12% sodium dodecyl sulfate–polyacrylamide gel electrophoresis (SDS–PAGE) and transferred to a polyvinylidene difluoride (PVDF) membrane (Millipore, Billerica, MA). The non-specific binding sites were blocked with TBST buffer [500 mM NaCl, 20 mM Tris–HCl (pH 7.4), and 0.4% Tween 20] containing 5% nonfat dry milk for 2 h at room temperature. Subsequently, the membranes were incubated overnight at 4 $^{\circ}$ C with specific primary antibodies diluted in TBST buffer containing 5% nonfat dry milk. Thereafter, the membranes were washed 3 times with TBST buffer and incubated at room temperature for 1 h with HRP-conjugated secondary antibody. After 3 wash with TBST buffer, the immunoblots were visualized by a Phototope-HRP Detection Kit (Cell Signaling, Danvers, MA) and exposed to a Kodak medical X-ray processor (Kodak, Rochester, NY).¹²

Subcellular Fractionation and Western Blot Analysis of Cytosolic Cytochrome c. After 3.5×10^6 cells/well were plated to a culture dish (100 \times 20 mm) for 24 h, the cells were treated for 36 h. Then, cells were harvested and washed twice with ice-cold PBS, suspended with 5-fold volume of ice-cold cell extract buffer [20 mM N-2-hydroxyethylpiperazine-N'-2-ethanesulfonic acid (HEPES)-KOH (pH 7.5), 10 mM KCl, 1.5 mM MgCl₂, 1 mM ethylenediaminetetraacetic acid (EDTA), 1 mM ethylene glycol bis(2-aminoethyl ether)-N,N,N',N'-tetraacetic acid (EGTA), 1 mM DTT, 250 mM sucrose, 0.1 mM phenylmethylsulfonyl fluoride (PMSF), and 0.02 mM aprotinin] and incubated for 40 min at 4 $^{\circ}$ C. Then, the cells were centrifuged at 110g for 10 min at 4 $^{\circ}$ C. The supernatant was subsequently centrifuged at 15000g for 15 min at 4 $^{\circ}$ C, and the final supernatant was used as the cytosolic fraction. Then, 5 \times loading buffer [250 mM Tris-Cl (pH 6.8), 50% glycerol, 10% sodium dodecyl sulfate, 1.25% bromphenol blue, and 0.5 M DTT] was added to the above obtained supernatant, and the mixture was boiled at 100 $^{\circ}$ C for 15 min. Thus, the protein solution was used for identification of cytosolic cytochrome c by immunoblotting with 10% SDS–PAGE and blotting

onto a PVDF membrane. The cytochrome *c* protein was detected using anti-cytochrome *c* antibody in the ratio of 1:1000.¹³

Statistical Analysis. Results were performed by *t* test or one-way analysis of variation (ANOVA) with SPSS 13.0 software (SPSS, Inc., Chicago, IL). Data were presented as the mean \pm standard error of the mean (SEM) of at least triplicate determinations. (*) $p < 0.05$ was indicative of a significant difference, and (**) $p < 0.01$ was indicative of a very significant difference. Densitometric analysis of western blot results was carried out by Image J [National Institutes of Health (NIH), Bethesda, MD].

RESULTS

Quercetin and Acacetin Showed Potent Cell Growth Inhibition of KB and KBv200 Cells. Results of cell viability assay experiments (Table 1) showed that quercetin and acacetin

Table 1. Cell Growth Inhibition Activity of Compounds 1–6

compounds	IC ₅₀ values (μ M)	
	KB	KBv200
apigenin (1)	>100	>100
acacetin (2)	49.04 \pm 3.64	41.33 \pm 6.05
kaempferol (3)	>100	>100
quercetin (4)	17.84 \pm 4.14	18.94 \pm 4.75
kaempferol 3-O-rhamnoside (5)	>100	>100
quercetin 3-O-rhamnoside (6)	>100	>100

were the most effective at inhibiting cell growth among the compounds tested. The IC₅₀ values of quercetin and acacetin against KB cells were 17.84 \pm 4.14 and 49.04 \pm 3.64 μ M ($p < 0.01$), respectively. The IC₅₀ values of quercetin and acacetin against KBv200 cells were 18.94 \pm 4.75 and 41.33 \pm 6.05 ($p <$

0.01), respectively. At the same time, quercetin and acacetin exhibited similar potency in KB and KBv200 cells ($p > 0.05$), respectively. Herein, quercetin exhibiting the most potent activity was selected to be investigated further.

Decrease of Intracellular ROS Level in KB and KBv200 Cells Induced by Quercetin. Quercetin has been reported to be antioxidant agents.¹⁴ Indeed, a decrease of ROS was observed after treatment of cells with this compound in our research. The results showed that quercetin induced a decrease of the ROS level in KB and KBv200 cells (Figure 2). After exposure to 15.0, 30.0, and 60.0 μ M quercetin for 24 h, the ROS level in KB cells was 88.22 \pm 6.60, 75.22 \pm 4.30, and 64.04 \pm 5.34% of the control, respectively. After exposure to 15.0, 30.0, and 60.0 μ M quercetin for 24 h, the ROS level in KBv200 cells was 86.66 \pm 1.78, 75.35 \pm 4.15, and 59.73 \pm 1.98% of the control, respectively.

Quercetin-Induced Loss of $\Delta\Psi$ m in KB and KBv200 Cells. DiOC6(3) was used as a mitochondrion-specific and voltage-dependent dye for determining $\Delta\Psi$ m, the loss of which is regarded as a limiting factor in the apoptotic pathway. Our results indicated that treatment with quercetin led to the loss of $\Delta\Psi$ m in KB and KBv200 cells (Figure 3). After KB cells were exposed to 15.0, 30.0, and 60.0 μ M quercetin for 24 h, $\Delta\Psi$ m was 91.54 \pm 4.29, 81.80 \pm 4.63, and 38.47 \pm 9.06% of the control, respectively. After KBv200 cells were exposed to 15.0, 30.0, and 60.0 μ M quercetin for 24 h, $\Delta\Psi$ m was 92.35 \pm 2.44, 76.68 \pm 7.28, and 38.22 \pm 7.35% of the control, respectively.

Release of Cytochrome *c* and Activation of Caspases Were Involved in the Apoptosis Induced by Quercetin. The mitochondrial pathway is one of the major apoptosis pathways, which is often related to the loss of $\Delta\Psi$ m. The

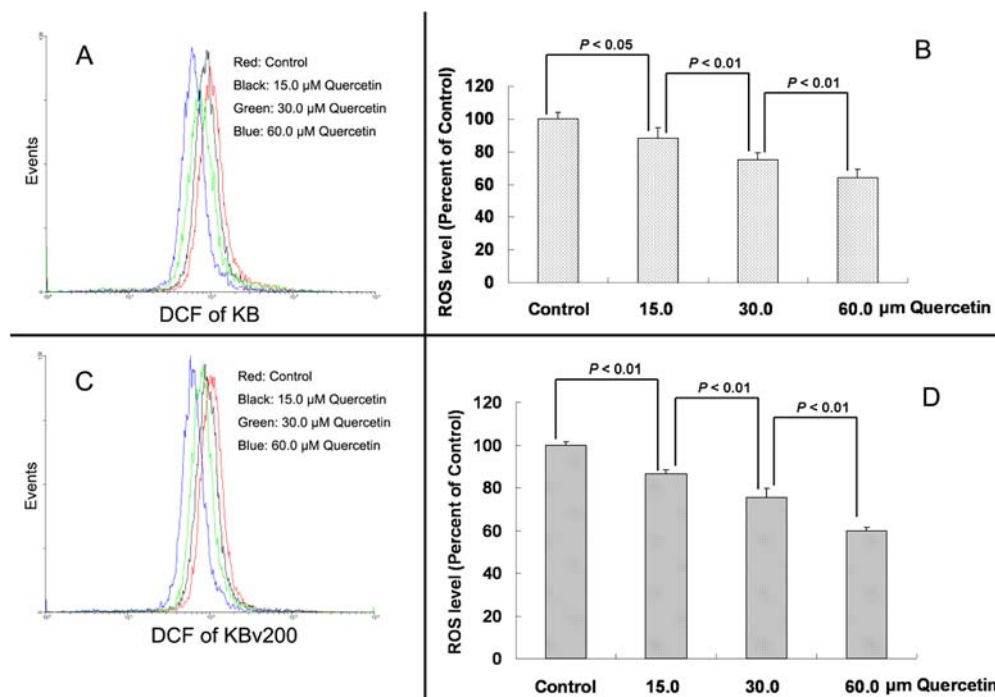


Figure 2. Quercetin decreased the intracellular ROS level of KB and KBv200 cells. After indicated cells were treated with 15.0, 30.0, and 60.0 μ M quercetin for 24 h, the ROS level was detected with DCF as a fluorescent probe. (A) Decrease of the ROS level in KB cells showing a concentration-dependent manner. (B) ROS levels in KB cells expressed as units of MFI were calculated as a percentage of the control. (C) Decrease of the ROS level in KBv200 cells showing a dose-related manner. (D) ROS levels in KBv200 cells expressed as units of MFI were calculated as a percentage of the control. Results were expressed as the mean \pm SEM of three determinations. $p < 0.05$ indicated a significant difference, and $p < 0.01$ indicated a very significant difference, versus the untreated control group or low concentrations of quercetin.

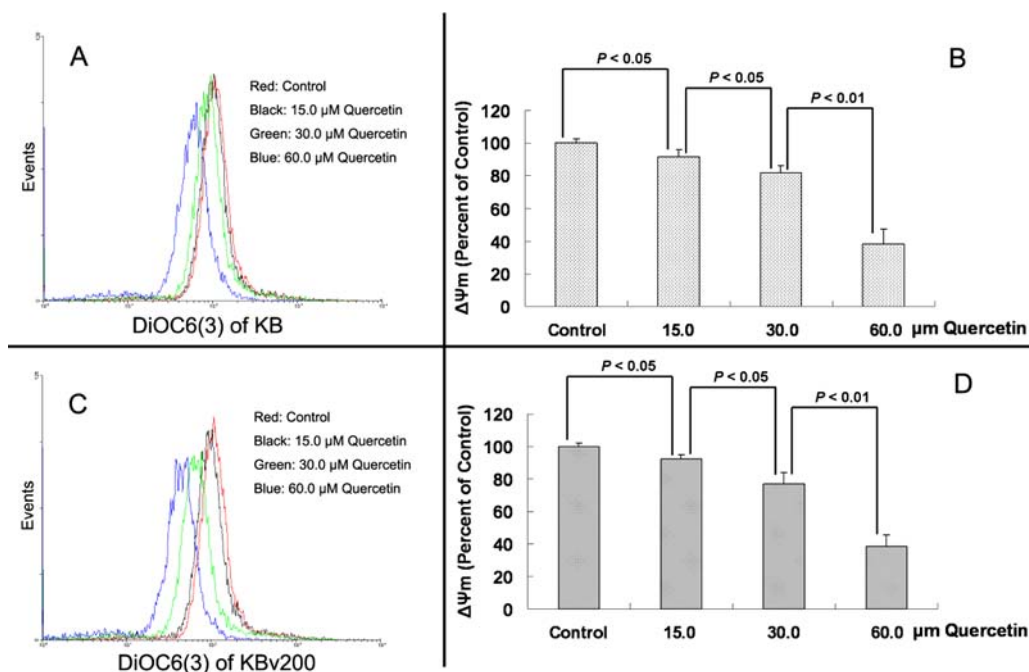


Figure 3. Quercetin decreased the $\Delta\Psi_m$ level of KB and KBv200 cells. After indicated cells were treated with 15.0, 30.0, and 60.0 μM quercetin for 24 h, the ROS level was detected with DiOC6(3) as a fluorescent probe. (A) Decrease of the $\Delta\Psi_m$ level in KB cells showing a dose-related manner. (B) ROS levels in KB cells expressed as units of MFI were calculated as a percentage of the control. (C) Decrease of the $\Delta\Psi_m$ level in KBv200 cells showing a concentration-dependent manner. (D) $\Delta\Psi_m$ levels in KBv200 cells expressed as units of MFI were calculated as a percentage of the control. Results were expressed as the mean \pm SEM of three determinations. $p < 0.05$ indicated a significant difference, and $p < 0.01$ indicated a very significant difference, versus the untreated control group or low concentrations of quercetin.

release of cytochrome *c* from the mitochondria to cytosol is the limiting factor in the mitochondrial pathway, and the loss of $\Delta\Psi_m$ has been suggested to cause the release of cytochrome *c*. The release of cytochrome *c* in a molecular weight of 14 kD can initiate apoptosis via the mitochondrial pathway by activation of caspase-9 and caspase-3 and by cleavage of PARP. The molecular weight of procaspase-9 was 47 kD, and the molecular weight of activated caspase-9 after cleavage was 37/35 kD. The molecular weight of procaspase-3 was 35 kD, and the molecular weight of activated caspase-3 was 17 kD. The molecular weight of PARP before and after cleavage was 116 and 89 kD, respectively.

After KB and KBv200 cells were treated with 15.0, 30.0, and 60.0 μM quercetin for 36 h, the release of cytochrome *c* increased in a concentration-corresponding manner (Figure 4). The ratios for densitometric values (cytochrome *c*/GAPDH) for control (0), 15.0, 30.0, and 60.0 μM quercetin were 0.11 ± 0.02 , 0.56 ± 0.04 , 0.79 ± 0.08 , and 1.08 ± 0.07 in KB cells, respectively. Those were 0.08 ± 0.01 , 0.33 ± 0.02 , 0.80 ± 0.02 , and 1.10 ± 0.02 in KBv200 cells, respectively.

Moreover, the activation of caspase-9 and caspase-3 and the cleavage of PARP in a dose-dependent manner were observed (Figure 5). Densitometric ratios of activated caspase-9/GAPDH for 0, 15.0, 30.0, and 60.0 μM quercetin/48 h in KB cells were 0.18 ± 0.05 , 0.39 ± 0.06 , 0.49 ± 0.04 , and 0.90 ± 0.11 , respectively. Densitometric ratios of activated caspase-3/GAPDH for 0, 15.0, 30.0, and 60.0 μM quercetin/48 h in KB cells were 0.14 ± 0.04 , 0.39 ± 0.04 , 0.48 ± 0.02 , and 0.59 ± 0.04 , respectively. Densitometric ratios of cleaved PARP/GAPDH for 0, 15.0, 30.0, and 60.0 μM quercetin/48 h in KB cells were 0.16 ± 0.02 , 0.48 ± 0.10 , 0.66 ± 0.03 , and 0.93 ± 0.08 , respectively. Densitometric ratios of activated caspase-9/GAPDH for 0, 15.0, 30.0, and 60.0 μM quercetin/48 h in

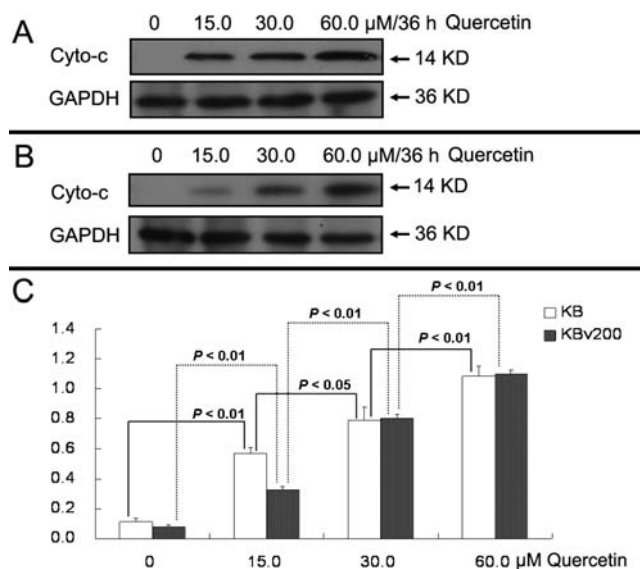


Figure 4. Quercetin treatment led to the release of cytochrome *c* of 14 kD in KB and KBv200 cells. After indicated cells were treated with 0, 15.0, 30.0, and 60.0 μM quercetin for 36 h, cytosolic cytochrome *c* was separated and determined. (A) Release of cytochrome *c* in KB cells. (B) Release of cytochrome *c* in KBv200 cells. (C) Densitometric analysis of western blot results of panels A and B. The values were calculated as (the gray density of desired blots of cytochrome *c*/the gray density of desired blots of GAPDH). The results were expressed as the mean \pm SEM of three experiments. $p < 0.05$ indicated a significant difference, and $p < 0.01$ indicated a very significant difference, versus the untreated control group or low concentrations of quercetin. GAPDH with a molecular weight of 36 kD detection was applied to confirm equal protein loading.

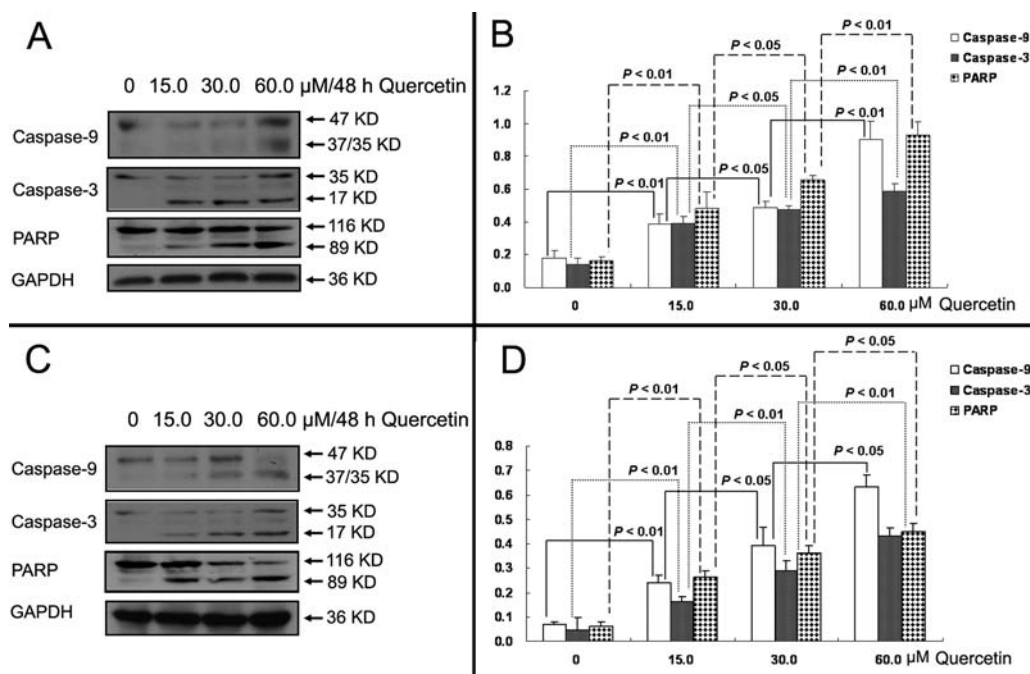


Figure 5. Quercetin treatment led to activation of caspase-9 and caspase-3 and cleavage of PARP. After KB and KBv200 cells were treated with 0, 15.0, 30.0, and 60.0 μM quercetin for 48 h, cells were collected and total protein was extracted. (A) Activation detection of caspase-9 and caspase-3 and cleavage of PARP in KB cells. (C) Activation detection of caspase-9 and caspase-3 and cleavage of PARP in KBv200 cells. (B and D) Densitometric analysis of western blot results of panels A and C, respectively. The values were calculated as (the gray density of desired blots regarding activated caspase-9 and caspase-3 and cleavage of PARP/the gray density of desired blots of GAPDH). The molecular weight of activated caspase-9 and caspase-3 were 37/35 and 17 kD, respectively. The molecular weight of cleaved PARP was 89 kD. The results were expressed as the mean \pm SEM of three experiments. $p < 0.05$ indicated a significant difference, and $p < 0.01$ indicated a very significant difference, versus the untreated control group or low concentrations of quercetin. GAPDH with a molecular weight of 36 kD detection was applied to confirm equal protein loading.

KBv200 cells were 0.07 ± 0.01 , 0.24 ± 0.03 , 0.39 ± 0.08 , and 0.63 ± 0.05 , respectively. Densitometric ratios of activated caspase-3/GAPDH for 0, 15.0, 30.0, and 60.0 μM quercetin/48 h in KBv200 cells were 0.05 ± 0.04 , 0.16 ± 0.02 , 0.29 ± 0.02 , and 0.43 ± 0.04 , respectively. Densitometric ratios of cleaved PARP/GAPDH for 0, 15.0, 30.0, and 60.0 μM quercetin/48 h in KBv200 cells were 0.06 ± 0.02 , 0.26 ± 0.03 , 0.36 ± 0.03 , and 0.45 ± 0.03 , respectively.

Quercetin-Induced Apoptosis in KB and KBv200 Cells Determined by Annexin V-FITC/PI. After exposure to 30.0 μM quercetin for 0, 12, and 24 h, KB and KBv200 cells were collected and exposed to Annexin V-FITC/PI double-staining and flow cytometry assay (Figure 6). The apoptosis rate for 0, 12, and 24 h was 6.80 ± 4.03 , 22.84 ± 1.34 , and $30.90 \pm 3.60\%$ in KB cells. The apoptosis rate for 0, 12, and 24 h was 5.67 ± 3.36 , 20.37 ± 1.80 , and $32.75 \pm 3.12\%$ in KBv200 cells.

Quercetin Did Not Change Expression of Bcl-2 or Bax. It has been reported that Bcl-2 and Bax play important roles in the mitochondrial pathway. A ratio increase of Bax expression to Bcl-2 expression will lead to apoptosis. Our research showed that expression of neither Bcl-2 nor Bax changed significantly in KB and KBv200 cells after treatment with quercetin for 48 h (Figure 7). Densitometric ratios of Bcl-2/GAPDH for 0, 15.0, 30.0, and 60.0 μM quercetin/48 h in KB cells were 0.71 ± 0.05 , 0.72 ± 0.09 , 0.72 ± 0.06 , and 0.78 ± 0.02 , respectively. Densitometric ratios of Bax/GAPDH for 0, 15.0, 30.0, and 60.0 μM quercetin/48 h in KB cells were 1.28 ± 0.07 , 1.30 ± 0.13 , 1.29 ± 0.11 , and 1.20 ± 0.06 , respectively. Densitometric ratios of Bcl-2/GAPDH for 0, 15.0, 30.0, and 60.0 μM quercetin/48 h in KBv200 cells were 1.01 ± 0.08 , 1.04 ± 0.02 , 0.98 ± 0.03 , and

0.98 ± 0.03 , respectively. Densitometric ratios of Bax/GAPDH for 0, 15.0, 30.0, and 60.0 μM quercetin/48 h in KBv200 cells were 0.79 ± 0.05 , 0.79 ± 0.03 , 0.75 ± 0.06 , and 0.80 ± 0.03 , respectively.

DISCUSSION

Cancer has become a public health problem of increasing importance because of its high rates of morbidity and mortality.¹⁵ Multi-drug resistance (MDR) is the main obstacle to the success of chemotherapy.¹⁶ Development of novel anticancer drugs taking effects in both sensitive and MDR cells is the available strategy of overcoming MDR. In this paper, quercetin was found to be effective in both sensitive KB and MDR KBv200 cells overexpressing ABCB1. Quercetin showed similar potency in KB and KBv200 cells ($p > 0.05$). It indicated that quercetin is effective in both sensitive cancer cells and ABCB1-induced MDR cancer cells. This provided one way of overcoming MDR.

Among these six flavanoids, quercetin is the most potent and acacetin is the second most potent. IC_{50} values of the other four flavanoids, namely, apigenin (1), kaempferol (3), kaempferol 3-*O*-rhamnoside (5), and quercetin 3-*O*-rhamnoside (6), were more than 100 μM . On the basis of the comparison of quercetin and quercetin 3-*O*-rhamnoside, the IC_{50} values indicated that glycoside at C-3 led to a decrease of anticancer activity. IC_{50} values of kaempferol and quercetin demonstrated that hydroxyl at C-3' was important to anticancer activity. Results of apigenin and acacetin implied that methoxy at C-4' was better than hydroxyl.

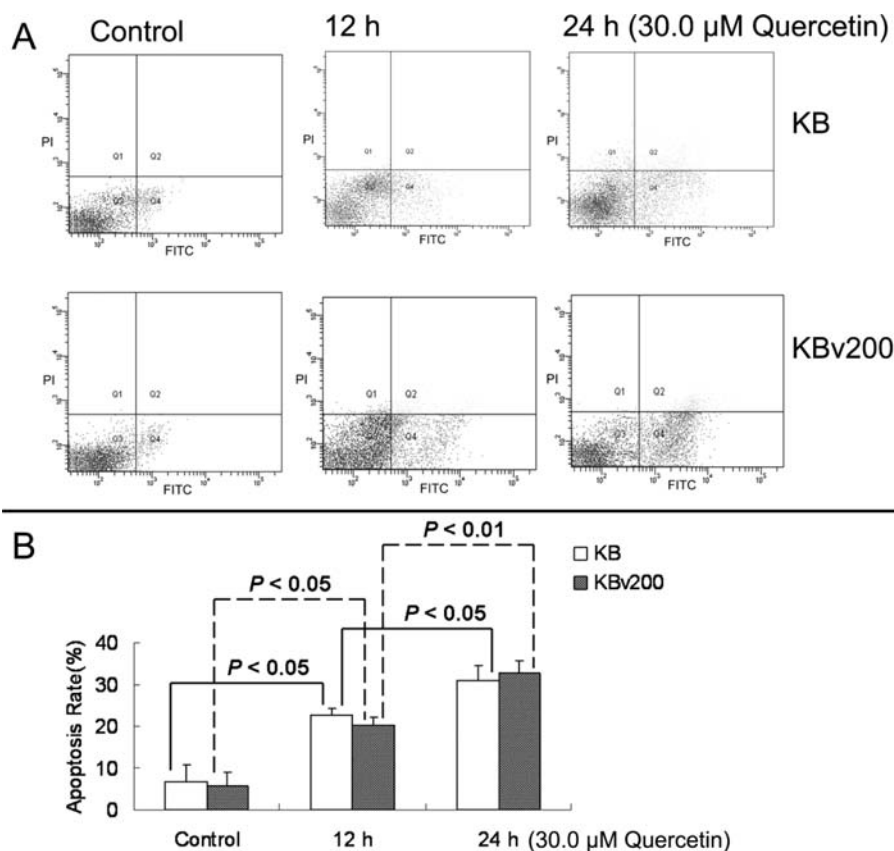


Figure 6. Quercetin-mediated cell apoptosis in KB and KBv200 cells was determined by Annexin V-FITC/PI double-staining and flow cytometer. (A) Time course of apoptosis in KB and KBv200 cells was explored after exposure to 30.0 μM quercetin for 0 (untreated control), 12, and 24 h. The bottom right quadrant represented cells stained mainly by Annexin V (early apoptotic cells), and the top right quadrant represented cells stained by both PI and Annexin V (late apoptotic/necrotic secondary necrosis). The top left quadrant represented cells stained mainly by PI, and the bottom left quadrant represented viable cells negative for both Annexin V and PI. (B) Apoptosis rate was shown in the bar graph. The apoptosis rate for the bottom right quadrant was expressed as the mean \pm SEM of three experiments. $p < 0.05$ indicated a significant difference, and $p < 0.01$ indicated a very significant difference.

As mentioned above, quercetin showed potent inhibition of cell growth in KB and KBv200 cells. Under our current understanding, apoptosis is the important mechanism via which many anticancer agents take their effects. Apoptosis is the highly controlled and organized death process regulating the development and homeostasis of multicellular organisms.¹⁷ Apoptosis is characterized by several well-defined processes, including the decrease in the cell volume, compaction of cytoplasmic organelles, condensation and fragmentation of nuclear chromatin, and activation of a family of cysteine proteases called caspase.¹⁸ The mitochondrial pathway plays an important role in apoptosis, among which cytochrome *c*, caspase-9, and caspase-3 were involved.¹⁹ Caspase-9 is activated after cytochrome *c* is released to cytosol and subsequent formation of the complex containing cytochrome *c*, apoptotic protease activation factor (Apaf)-1, and procaspase-9.^{20,21} Caspase-9 can activate downstream caspases, including caspase-7 and caspase-3, that eventually lead to apoptosis.²²

Herein, our results demonstrated that quercetin treatment led to the release of cytochrome *c* (Figure 4). Also, activation of caspase-9 and caspase-3 and cleavage of PARP were observed in KB and KBv200 cells (Figure 5). Moreover, apoptosis determined by Annexin V-FITC-PI Detection Kit confirmed the fact that quercetin could induce apoptosis in KB and KBv200 cells (Figure 6). These results indicated that quercetin could induce apoptosis via the mitochondrial pathway.

It is well-known that an increase of intracellular ROS can lead to apoptosis. On the other hand, a decrease of ROS can also ruin the stability of mitochondria, which is followed by a loss of $\Delta\Psi\text{m}$, release of cytochrome *c* into cytosol, and cascade activation of caspases.^{10,23} It has been reported that Bcl-2 and Bax play an important role in causing apoptosis through the mitochondrial pathway.^{23,24} Granado-Serrano et al. reported that quercetin could downregulate Bcl-2 in HepG2 cells.²⁵ In our research, the expression of Bcl-2 and Bax did not change after quercetin treatment. It implied that apoptosis of KB and KBv200 cells induced by quercetin was not related to upregulation of Bax or downregulation of Bcl-2.

The mitogen-activated protein kinase (MAPK) signal pathway has been proven to play a role in pharmacological mechanisms. However, there are different opinions on how quercetin influences the MAPK pathway. Granado-Serrano et al. showed that quercetin could activate p38 MAPK by a dose-dependent manner from 5 to 50 μM .²⁶ Liu et al. reported that quercetin attenuated ethanol-induced oxidative stress through a pathway that involves extracellular signal-regulated kinase (ERK) activation and HO-1 upregulation.²⁷ Ahn et al. showed that quercetin induces adipocyte apoptosis by inhibiting the MAPK pathway.²⁸ Choi et al. reported that quercetin inhibits the activation of p38 MAPK induced by Cu^{2+} -oxidized low-density lipoprotein (LDL) in human umbilical vein endothelial cells (HUVEC).²⁹ Xavier et al. showed that quercetin inhibits

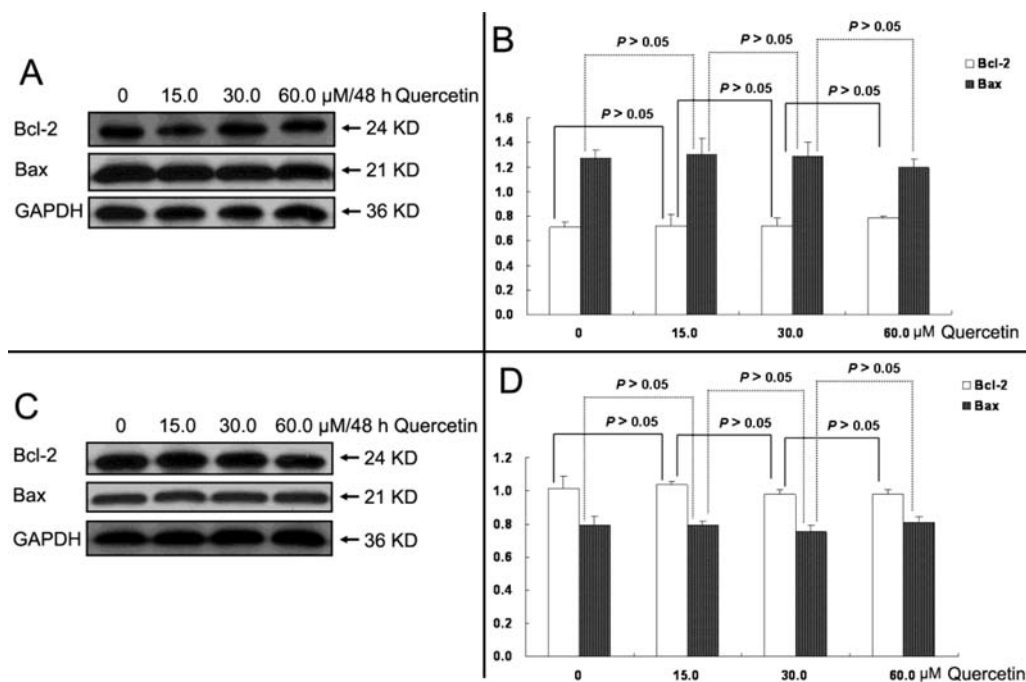


Figure 7. Quercetin did not affect the expression of Bcl-2 and Bax. After indicated cells were treated with 0, 15.0, 30.0, and 60.0 μM quercetin for 48 h, the protein expression of Bcl-2 and Bax in KB and KBv200 cells was detected. (A) Expression of Bcl-2 and Bax in KB cells. (B) Densitometric analysis of western blot results of panel A expressed as the mean \pm SEM of three experiments. (C) Expression of Bcl-2 and Bax in KBv200 cells. (D) Densitometric analysis of western blot results of panel C expressed as the mean \pm SEM of three experiments. $p < 0.05$ indicated a significant difference, and $p < 0.01$ indicated a very significant difference. GAPDH with a molecular weight of 36 kDa detection was applied to confirm equal protein loading.

phospho-ERK expression in HCT15 and CO115 cells.³⁰ Herein, the relation between mitochondrial pathway apoptosis and the MAPK pathway was not investigated in our research.

Another important issue is whether the quercetin level *in vivo* can reach the effective concentration. Other authors have paid attention to the *in vivo* process in rats after oral administration of quercetin. In rats fed with a 0.1% quercetin diet for 11 weeks, the concentration of quercetin in plasma was 7.7 μM . In rats fed with a 1% quercetin diet for 11 weeks, the concentration of quercetin in plasma was 40.4 μM .⁶ Interestingly, chronic ingestion of apple pectin can enhance the absorption of quercetin. Pectin, a major type of dietary fiber, is widely distributed in fruits and vegetables, mainly citrus fruits and apples.³¹ Thus, it is possible for quercetin to reach the effective concentration *in vivo*.

To summarize, in this work, we investigated the anticancer effects of six flavonoids. Quercetin was the most potent among these six compounds. Also, quercetin induced apoptosis in KB and KBv200 cells via the mitochondrial pathway. Our research provides information for the pharmacological effect and daily diet of quercetin.

AUTHOR INFORMATION

Corresponding Author

*E-mail: hbchen@hkbu.edu.hk.

Funding

This research was funded by the General Research Fund of Hong Kong (HKBU-260111).

Notes

The authors declare no competing financial interest.

ABBREVIATIONS USED

MTT, 3-(4,5-dimethyl-2-thiazolyl)-2,5-diphenyl-2H-tetrazolium bromide; DiOC6(3), 3,3'-dihexyloxycarbocyanine iodide; DCFH-DA, 2',7'-dichlorofluorescein diacetate; VCR, vincristine; P-gp (ABCB1), P-glycoprotein; ROS, reactive oxygen species; DCF, 2',7'-dichlorofluorescein; PARP, poly (ADP-ribose) polymerase; MDR, multi-drug resistance

REFERENCES

- (1) Cooper, E. L. Drug discovery, CAM and natural products. *J. Evidence-Based Complementary Altern. Med.* **2004**, *1*, 215–217.
- (2) Wesolowska, O. Interaction of phenothiazines, stilbenes and flavonoids with multidrug resistance-associated transporters, P-glycoprotein and MRP1. *Acta Biochim. Pol.* **2011**, *58*, 433–448.
- (3) Kandaswami, C.; Lee, L. T.; Lee, P. P.; Hwang, J. J.; Ke, F. C.; Huang, Y. T.; Lee, M. T. The antitumor activities of flavonoids. *In Vivo* **2005**, *19*, 895–909.
- (4) Egert, S.; Rimbach, G. Which sources of flavonoids: Complex diets or dietary supplements? *Adv. Nutr.* **2011**, *2*, 8–14.
- (5) Dawa, Z.; Bai, Y.; Zhou, Y.; Gesang, S. A. P.; Ding, L. Chemical constituents of the whole plants of *Saussurea medusa*. *J. Nat. Med.* **2009**, *63*, 327–330.
- (6) de Boer, V. C.; Dihal, A. A.; van der Woude, H.; Arts, I. C.; Wolfram, S.; Alink, G. M.; Rietjens, I. M.; Keijer, J.; Hollman, P. C. Tissue distribution of quercetin in rats and pigs. *J. Nutr.* **2005**, *135*, 1718–1725.
- (7) Yi, T.; Lo, H. W.; Zhao, Z. Z.; Yu, Z. L.; Yang, Z. J.; Chen, H. B. Comparison of the chemical composition and pharmacological effects of the aqueous and ethanolic extracts from a Tibetan "Snow Lotus" (*Saussurea laniceps*) herb. *Molecules* **2012**, *17*, 7183–7194.
- (8) Yi, T.; Chen, H. B.; Zhao, Z. Z.; Jiang, Z. H.; Cai, S. Q.; Wang, T. M. Comparative analysis of the major constituents in the traditional Tibetan medicinal plants *Saussurea laniceps* and *S. medusa* by LC–DAD–MS. *Chromatographia* **2009**, *70*, 957–962.

- (9) Yi, T.; Chen, H. B.; Zhao, Z. Z.; Jiang, Z. H.; Cai, S. Q.; Wang, T. M. Identification and determination of the major constituents in the traditional Uighur medicinal plant *Saussurea involucreta* by LC–DAD–MS. *Chromatographia* **2009**, *69*, 537–542.
- (10) Zhang, J. Y.; Wu, H. Y.; Xia, X. K.; Liang, Y. J.; Yan, Y. Y.; She, Z. G.; Lin, Y. C.; Fu, L. W. Anthracenedione derivative 1403P-3 induces apoptosis in KB and KBv200 cells via reactive oxygen species-independent mitochondrial pathway and death receptor pathway. *Cancer Biol. Ther.* **2007**, *6*, 1413–1421.
- (11) Zhang, J. Y.; Liang, Y. J.; Chen, H. B.; Zheng, L. S.; Mi, Y. J.; Wang, F.; Zhao, X. Q.; Wang, X. K.; Zhang, H.; Fu, L. W. Structure identification of Euphorbia factor L3 and its induction of apoptosis through the mitochondrial pathway. *Molecules* **2011**, *16*, 3222–3231.
- (12) Yan, Y. Y.; Zheng, L. S.; Zhang, X.; Chen, L. K.; Singh, S.; Wang, F.; Zhang, J. Y.; Liang, Y. J.; Dai, C. L.; Gu, L. Q.; Zeng, M. S.; Talele, T. T.; Chen, Z. S.; Fu, L. W. Blockade of Her2/neu binding to Hsp90 by emodin azide methyl anthraquinone derivative induces proteasomal degradation of Her2/neu. *Mol. Pharm.* **2011**, *8*, 1687–1697.
- (13) Zhang, J. Y.; Tao, L. Y.; Liang, Y. J.; Chen, L. M.; Mi, Y. J.; Zheng, L. S.; Wang, F.; She, Z. G.; Lin, Y. C.; To, K. K.; Fu, L. W. Anthracenedione derivatives as anticancer agents isolated from secondary metabolites of the mangrove endophytic fungi. *Mar. Drugs* **2010**, *8*, 1469–1481.
- (14) Bubols, G. B.; Vianna, D. D.; Medina-Remón, A.; von Poser, G.; Lamuela-Raventos, R. M.; Eifler-Lima, V. L.; Garcia, S. C. The antioxidant activity of coumarins and flavonoids. *Mini-Rev. Med. Chem.* **2012** (Epub ahead of print).
- (15) Zhang, J. Y.; Tao, L. Y.; Liang, Y. J.; Yan, Y. Y.; Dai, C. L.; Xia, X. K.; She, Z. G.; Lin, Y. C.; Fu, L. W. Secalonic acid D induced leukemia cell apoptosis and cell cycle arrest of G(1) with involvement of GSK-3 β / β -catenin/c-Myc pathway. *Cell Cycle* **2009**, *8*, 2444–2450.
- (16) Zhang, J. Y.; Mi, Y. J.; Chen, S. P.; Wang, F.; Liang, Y. J.; Zheng, L. S.; Shi, C. J.; Tao, L. Y.; Chen, L. M.; Chen, H. B.; Fu, L. W. Euphorbia factor L1 reverses ABCB1-mediated multidrug resistance involving interaction with ABCB1 independent of ABCB1 down-regulation. *J. Cell Biochem.* **2011**, *112*, 1076–1083.
- (17) Yan, Y.; Su, X.; Liang, Y.; Zhang, J.; Shi, C.; Lu, Y.; Gu, L.; Fu, L. Emodin azide methyl anthraquinone derivative triggers mitochondrial-dependent cell apoptosis involving in caspase-8-mediated Bid cleavage. *Mol. Cancer Ther.* **2008**, *7*, 1688–1697.
- (18) Chiu, T. L.; Su, C. C. Tanshinone IIA induces apoptosis in human lung cancer A549 cells through the induction of reactive oxygen species and decreasing the mitochondrial membrane potential. *Int. J. Mol. Med.* **2010**, *25*, 231–236.
- (19) Fulda, S. Modulation of mitochondrial apoptosis by PI3K inhibitors. *Mitochondrion* **2012** (Epub ahead of print).
- (20) Choi, S. H.; Ahn, J. B.; Kim, H. J.; Im, N. K.; Kozukue, N.; Levin, C. E.; Friedman, M. Changes in free amino acid, protein, and flavonoid content in jujube (*Ziziphus jujube*) fruit during eight stages of growth and antioxidative and cancer cell inhibitory effects by extracts. *J. Agric. Food Chem.* **2012**, *60*, 10245–10255.
- (21) Quan, Z.; Gu, J.; Dong, P.; Lu, J.; Wu, X.; Wu, W.; Fei, X.; Li, S.; Wang, Y.; Wang, J.; Liu, Y. Reactive oxygen species-mediated endoplasmic reticulum stress and mitochondrial dysfunction contribute to cirsimaritin-induced apoptosis in human gallbladder carcinoma GBC-SD cells. *Cancer Lett.* **2010**, *295*, 252–259.
- (22) Moon, H. S.; Lim, H.; Moon, S.; Oh, H. L.; Kim, Y. T.; Kim, M. K.; Lee, C. H. Benzylidihydroxyoctenone, a novel anticancer agent, induces apoptosis via mitochondrial-mediated pathway in androgen-sensitive LNCaP prostate cancer cells. *Bioorg. Med. Chem. Lett.* **2009**, *19*, 742–744.
- (23) Wang, X. H.; Jia, D. Z.; Liang, Y. J.; Yan, S. L.; Ding, Y.; Chen, L. M.; Shi, Z.; Zeng, M. S.; Liu, G. F.; Fu, L. W. Lgf-YL-9 induces apoptosis in human epidermoid carcinoma KB cells and multidrug resistant KBv200 cells via reactive oxygen species-independent mitochondrial pathway. *Cancer Lett.* **2007**, *249*, 256–270.
- (24) Skommer, J.; Brittain, T.; Raychaudhuri, S. Bcl-2 inhibits apoptosis by increasing the time-to-death and intrinsic cell-to-cell variations in the mitochondrial pathway of cell death. *Apoptosis* **2010**, *15*, 1223–1233.
- (25) Granado-Serrano, A. B.; Martín, M. A.; Bravo, L.; Goya, L.; Ramos, S. Quercetin induces apoptosis via caspase activation, regulation of Bcl-2, and inhibition of PI-3-kinase/Akt and ERK pathways in a human hepatoma cell line (HepG2). *J. Nutr.* **2006**, *136*, 2715–2721.
- (26) Granado-Serrano, A. B.; Martín, M. A.; Bravo, L.; Goya, L.; Ramos, S. Quercetin modulates Nrf2 and glutathione-related defenses in HepG2 cells: Involvement of p38. *Chem.-Biol. Interact.* **2012**, *195*, 154–164.
- (27) Liu, S.; Hou, W.; Yao, P.; Li, N.; Zhang, B.; Hao, L.; Nüssler, A. K.; Liu, L. Heme oxygenase-1 mediates the protective role of quercetin against ethanol-induced rat hepatocytes oxidative damage. *Toxicol. In Vitro* **2012**, *26*, 74–80.
- (28) Ahn, J.; Lee, H.; Kim, S.; Park, J.; Ha, T. The anti-obesity effect of quercetin is mediated by the AMPK and MAPK signaling pathways. *Biochem. Biophys. Res. Commun.* **2008**, *373*, 545–549.
- (29) Choi, J. S.; Kang, S. W.; Li, J.; Kim, J. L.; Bae, J. Y.; Kim, D. S.; Shin, S. Y.; Jun, J. G.; Wang, M. H.; Kang, Y. H. Blockade of oxidized LDL-triggered endothelial apoptosis by quercetin and rutin through differential signaling pathways involving JAK2. *J. Agric. Food Chem.* **2009**, *57*, 2079–2086.
- (30) Xavier, C. P.; Lima, C. F.; Preto, A.; Seruca, R.; Fernandes-Ferreira, M.; Pereira-Wilson, C. Luteolin, quercetin and ursolic acid are potent inhibitors of proliferation and inducers of apoptosis in both KRAS and BRAF mutated human colorectal cancer cells. *Cancer Lett.* **2009**, *281*, 162–170.
- (31) Nishijima, T.; Iwai, K.; Saito, Y.; Takida, Y.; Matsue, H. Chronic ingestion of apple pectin can enhance the absorption of quercetin. *J. Agric. Food Chem.* **2009**, *57*, 2583–2587.